Influence of ENSO on precipitation in the East River basin, south China

Qiang Zhang,[1,2,3] Jianfeng Li,[4] Vijay P. Singh,[5] Chong-Yu Xu,[6] and Jingyun Deng[1,2,3]

Received 11 September 2012; revised 4 February 2013; accepted 16 February 2013.

[1] A majority of the literature analyzing the role of El Niño–Southern Oscillation (ENSO) and other teleconnections has focused on summer precipitation and on global and regional scales. Seasonal precipitation, occurring at local scale ($<50{,}000$ km^2; i.e., a size of one grid cell of a typical global climate model), is of considerable importance for flood mitigation, water supply, and water resources management. In view of the relative absence of studies exploring the forces driving local precipitation, the present study examines this precipitation regime (represented by monthly precipitation data for a period of 1956–2005 from 21 gauge stations in the East River basin) as a response to well-known determining factors, i.e., Southern Oscillation Index (SOI), El Niño Modoki index (EMI), and sea surface temperature anomalies (SSTA) of Niño 1 + 2, Niño 3, Niño 4, and Niño 3.4. To achieve the goal of the study, three types of ENSO events were defined: eastern Pacific warming (EPW), central Pacific warming (CPW), and eastern Pacific cooling (EPC). Mann–Whitney *U* test was applied to assess whether the probabilistic behavior of precipitation in the ENSO period was different from that in the normal period. The Pearson correlation coefficient was calculated to investigate the relations between areal precipitation in the East River basin and the above-mentioned ENSO indices. Results indicated that (1) EPW caused more precipitation in autumn and winter, but less precipitation in summer. EPW even brought about extremely heavy precipitation in summer and winter. (2) CPW caused less precipitation in spring, autumn, and the annual totals. Sometimes, CPW might bring about heavy precipitation. The precipitation pattern in summer in CPW was different from the normal years. (3) EPC caused more precipitation in autumn and less precipitation in spring and winter. The middle East River basin is the region where precipitation has decreased most severely due to EPC. (4) SSTA, SOI, and EMI had significant relations with areal precipitation from January to March. EMI is the only index having significant correlation with precipitation in April.

Citation: Zhang, Q., J. Li, V. P. Singh, C.-Y. Xu, and J. Deng (2013), Influence of ENSO on precipitation in the East River basin, south China, *J. Geophys. Res. Atmos.*, *118*, doi:10.1002/jgrd.50279.

1. Introduction

[2] Understanding and quantification of the relationship between regional climate anomaly and large-scale circulation have been a hot topic in the global research community. Of which, the influence of El Niño–Southern Oscillation (ENSO) on climate in the Asia/Pacific Region and influence of the North Atlantic Oscillation on climate in Europe have drawn much attention in recent years [*Power et al.*, 1999; *Wang et al.*, 2000; *Wrzesi ski and Paluszkiewicz*, 2011; *Gelati et al.*, 2011; *Parry et al.*, 2012; *Skaugen et al.*, 2012]. El Niño–Southern Oscillation (ENSO) is a well-recognized phenomenon that takes place across the tropical Pacific Ocean and remarkably influences the climate change around the world. ENSO can trigger occurrences of extreme hydroclimatological events, such as floods, droughts, and cyclones [*Cole and Cook*, 1998; *Andrews et al.*, 2004; *Zhang et al.*, 2007]. These extreme events may cause huge socio-economic losses [*Nicholls*, 1985; *Power et al.*, 1999; *Zhang et al.*, 2012a]. During the past 150 years, damages worth $800 million/year have been attributed to El Niño and damages worth $1600 million/year to La Niña in the United States alone [*Kim et al.*, 2009; *Pielke and Landsea*, 1999]. It is therefore not surprising that the influence of ENSO on weather and hydrological extreme events has been receiving

[1]Department of Water Resources and Environment, Sun Yat-sen University, Guangzhou, China.
[2]Key Laboratory of Water Cycle and Water Security in Southern China of Guangdong High Education Institute, Sun Yat-sen University, Guangzhou, China.
[3]School of Geography and Planning, and Guangdong Key Laboratory for Urbanization and Geo-simulation, Sun Yat-sen University, Guangzhou, China.
[4]Department of Geography and Resource Management, The Chinese University of Hong Kong, Hong Kong, China.
[5]Department of Biological and Agricultural Engineering and Department of Civil and Environmental Engineering, Texas A&M University, College Station, Texas, USA.
[6]Department of Geosciences, University of Oslo, Oslo, Norway.

Corresponding author: Q. Zhang, Department of Water Resources and Environment, Sun Yat-sen University, Guangzhou 510275, China. (zhangq68@mail.sysu.edu.cn)

2169-897X/13/10.1002/jgrd.50279

increasing concerns from hydrometeorologists and policy-makers [e.g., *Wang et al*., 2000; *Ratnam et al*., 2012].

[3] The influence of ENSO on global and regional climate has been widely investigated in recent years. *Kumar et al*. [1999] studied 140 year historical data and concluded that the negative correlation between ENSO and the Indian summer monsoon had collapsed in recent years. *Wang et al*. [2000] investigated how ENSO influenced East Asian climate, and presented observations as evidence to show the teleconnection between the central Pacific and East Asia. *Eichler and Higgins* [2006] used six hourly sea level pressure data during 1950–2002 from the National Centers for Environmental Prediction–National Center for Atmospheric Research reanalysis and European Centre for Medium-Range Weather Forecasts 40 year reanalysis (ERA-40) data from 1971–2000 to examine the variations of North American extratropical cyclones. *Dai and Wigley* [2000] used satellite estimates of oceanic precipitation and observed rain gauge records to obtain a global climatology of ENSO-induced precipitation anomalies.

[4] Recently, an anomalous sea surface temperature anomaly (SSTA) pattern different from typical El Niño event, called El Niño Modoki, was identified [*Ashok et al*., 2007]. El Niño Modoki is characterized by warm sea surface temperature anomaly in the central tropical Pacific and cold sea surface temperature anomaly in the eastern and western Pacific [*Ashok et al*., 2007, 2009]. The differences in teleconnections between El Niño and El Niño Modoki have been analyzed in many studies. *Taschetto and England* [2008] found that the maximum rainfall occurred in austral autumn during Modoki but in austral spring during classical El Niño. They also concluded that a significant reduction in precipitation over northeastern and southeastern Australia was associated with the classical El Niño, while a reduction over northwestern and northern Australia was associated with Modoki. *Ashok et al*. [2009] applied historical data since 1979 to investigate the 2004 El Niño Modoki event, and showed that this event was associated with distinct equatorial coupled ocean-atmosphere dynamics different from the classical El Niño. *Ratnam et al*. [2012] studied the El Niño Modoki during boreal winter of 2009 and indicated that El Niño Modoki accounted for most of the anomalous situations over North America, Europe, and most countries in the Southern Hemisphere.

[5] How ENSO impacts precipitation in China has been investigated previously. *Zhang et al*. [1999] showed that El Niño significantly affected precipitation in China. *Zhang et al*. [2007] studied the relationship between annual maximum streamflow in the Yangtze River basin and ENSO, and showed that in-phase relations were detected in the lower Yangtze River basin and antiphase relations were found in the upper Yangtze River basin. *Feng et al*. [2011a] studied the differences in the impact of El Niño and El Niño Modoki on precipitation in China in decaying phases and indicated that precipitation responded to El Niño and El Niño Modoki differently in various areas in different seasons. Above literature survey reveals that relatively less attention has been paid on exploring the forces driving local precipitation in a scale of $<50{,}000$ km^2, which is of considerable importance for flood mitigation, water supply, and water resources management.

[6] The East River is a crucial tributary of the Pearl River, which is the third largest river in China and is located in southeastern China (Figure 1). Concurrent with the rapid increase in population and booming economic development in the Pearl River Delta region, the East River basin has become an important source of water resources for society, agriculture, commerce, and industry [*Chen et al*., 2011]. Recently, 80% of Hong Kong's annual water demands is provided by the East River basin [*Chen*, 2001]. Moreover, the variability and availability of water resources of the East River basin are closely related to precipitation changes. Hence, it is vital to study how precipitation in the East River basin responds to different ENSO events. Although many

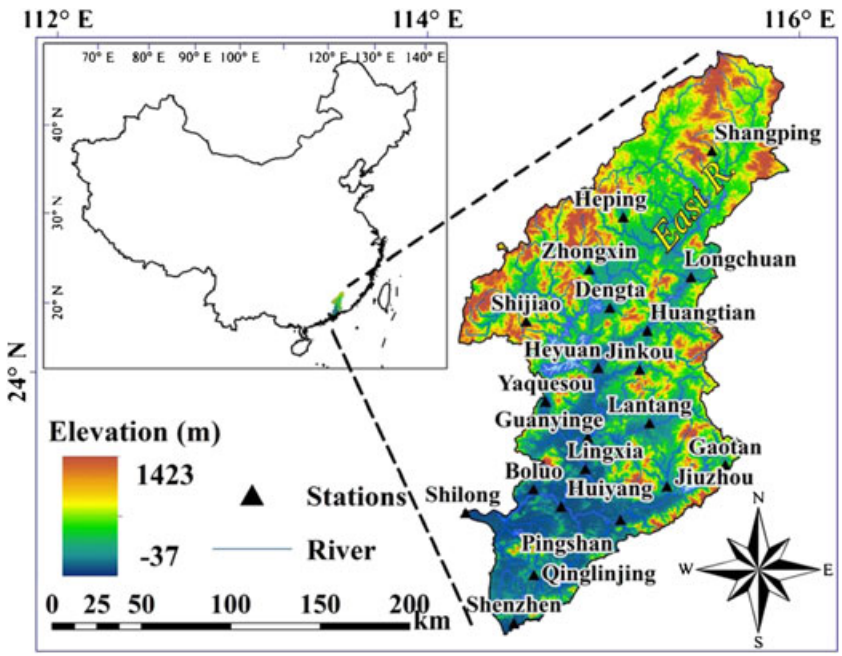

Figure 1. Rain gauges in the East River basin.

studies have investigated the impacts of ENSO events on a large scale, such as over East Asia and China, no systematic study on the impact of ENSO events on the East River basin has been carried out. Exploring precipitation characteristics in the East River basin stemming from different ENSO events can help to understand how climate in the East River basin changes with ENSO and help to compare precipitation variations in the East River basin with regional precipitation changes in other parts of the world.

[7] Therefore, the objectives of this paper were as follows: (1) to investigate temporal and spatial anomalies of precipitation in the East River basin; (2) to study the characteristics of precipitation in the East River basin during classical El Niño, La Niña, and El Niño Modoki events; and (3) to analyze the correlation between precipitation and various ENSO indices. This study not only helps to understand the precipitation variations in the East River basin during various ENSO periods but also provides useful references for similar studies in other regions of the world.

2. Data

[8] Monthly precipitation for a period of 1956–2005 from 21 rainy gauges in the East River basin, China, was used (Figure 1). Details of the monthly precipitation data are listed in Table 1. Among these stations, missing values were found at the Shijiao, Shangping, and Yaquesou stations. The missing values were interpolated based on the contours of monthly precipitation. The Thiessen method [*Pardo-Iguzquiza*, 1998] was applied to calculate the areal precipitation in the East River basin.

[9] The sea surface temperature anomalies (SSTA) of Niño 1 + 2 (0–10°S, 90–80°W), Niño 3 (5°N–5°S, 150–90°W), Niño 4 (5°N–5°S, 160°E–90°W), and Niño 3.4 (5°N–5°S, 170–120°W) were calculated using the Extended Reconstructed Sea Surface Temperature version 3 (ERSST. v3) [*Smith et al*., 2008]. The Southern Oscillation Index (SOI), released by Australian Government Bureau of Meteorology as an index reflecting the development and intensity of El Niño and La Niña events, was obtained. The El Niño Modoki index (EMI), an indication of El Niño Modoki events (Pseudo El Niño), was also computed [*Ashok et al*., 2007]. The SSTA and the above indices are commonly used indications of El Niño, El Niño Modoki, and La Niña events and were employed in this study.

[10] *Kim et al*. [2009] classified the ENSO events into three types: eastern Pacific warming (EPW), central Pacific warming (CPW), and eastern Pacific cooling (EPC). These events were defined by the detrended sea surface temperature [*Smith and Reynolds*, 2004] anomaly index for August to October. The definitions of EPW, CPW, and EPC events are as follows: for EPW, Niño 3 warming larger than 1 standard deviation (SD); for EPC, Niño 3 or Niño 3.4 cooler than 1 SD; for CPW, Niño 4 warming larger than 1 SD, while Niño 3 stays below this range. The classification of EPW, CPW, and EPC is shown in Table 2. The years without any type of ENSO events are termed as normal years. In addition, it should be noted that CPW events amount to El Niño Modoki events.

Table 1. Details of Rainy Gauges in the East River Basin

No.	Station	Longitude (E)	Latitude (N)	Missing Value
1	Boluo	114.283	23.183	N/A
2	Dengta	114.8	24.017	N/A
3	Gaotan	115.3	23.183	N/A
4	Guanyinge	114.6	23.4	N/A
5	Heping	114.933	24.45	N/A
6	Heyuan	114.7	23.733	N/A
7	Huangtian	114.983	23.883	N/A
8	Huiyang	114.417	23.083	N/A
9	Jinkou	114.917	23.7	N/A
10	Jiuzhou	114.983	23.117	N/A
11	Lantang	114.933	23.433	N/A
12	Lingxia	114.567	23.25	N/A
13	Longchuan	115.25	24.117	N/A
14	Pingshan	114.717	22.983	N/A
15	Qinglinjing	114.233	22.767	N/A
16	Shangping	115.45	24.717	2001–2002
17	Shenzhen	114.1	22.55	N/A
18	Shijiao	114.35	24	2003–2005
19	Shilong	113.867	23.1	N/A
20	Yaquesou	114.4	23.6	1989
21	Zhongxin	114.717	24.217	N/A

3. Methodology

[11] In this study, the Mann–Whitney *U* test is applied to detect whether the statistical behavior of two precipitation series in different ENSO years is the same; the Pearson correlation analysis is used to examine the linear relationship between observed precipitation and various ENSO indices; and the precipitation anomaly index is used to indicate how the precipitation in a specific ENSO period deviates from the precipitation in the normal period. For the sake of completeness, the methods and the index are briefly described in the following subsections.

3.1. Mann–Whitney *U* Test

[12] The Mann–Whitney *U* test, a rank sum test, is a nonparametric statistical test for assessing whether series x and y are independent samples from different continuous distributions [*Mann and Whitney*, 1947; *Zhang et al*., 2012b]. Let x denote precipitation series in the year under a type of ENSO event (EPW, CPW, EPC, or normal), and let y denote precipitation series under another type of ENSO event. Then, let the distribution functions of series x and y be f and g, respectively. The two series are extracted from f and g with sample sizes of n and m, respectively. Then, the null hypothesis is: $f = g$.

[13] The statistic of the Mann–Whitney *U* test is z. The significance level in this study is $\alpha = 0.05$, and Mann–Whitney *U* test performed in this study is two sided, so the significant threshold of z is $Z_{1-\alpha/2} = 1.96$. If $|z| \le Z_{1-\alpha/2}$, then the statistical distributions of two precipitation series from different ENSO periods are identical. If $|z| > Z_{1-\alpha/2}$, then the statistical behavior of the two precipitation series from different ENSO periods is significantly different.

Table 2. Years of EPW, CPW and EPC

ENSO Event	Years
EPW	1957, 1963, 1965, 1972, 1976, 1982, 1987, 1997
CPW	1969, 1991, 1994, 2002, 2004
EPC	1964, 1970, 1971, 1973, 1975, 1985, 1988, 1995, 1998, 1999

3.2. Pearson Correlation

[14] The linear correlation between series x and y can be represented by the Pearson correlation [*Zou et al.*, 2003]. The Pearson linear correlation coefficient r can be calculated as follows:

$$r = \frac{\sum_{i=1}^{n}(x_i - \bar{x})(y_i - \bar{y})}{\sqrt{\sum_{i=1}^{n}(x_i - \bar{x})^2 \sum_{i=1}^{n}(y_i - \bar{y})^2}} \quad (1)$$

where n is the size of the series; x_i and y_i ($i = 1, \ldots, n$) are the values of x and y, respectively; and $\bar{x}$ and $\bar{y}$ are the sample means of x and y. Furthermore, the two-sided t test under the 0.05 significance level was used to assess whether r is significantly different from zero.

3.3. Precipitation Anomaly Index

[15] In a specific ENSO period, the precipitation anomaly index is defined as follows:

$$D_{ij} = \frac{\overline{\mathrm{PE}_{ij}} - \overline{\mathrm{PN}_{ij}}}{\overline{\mathrm{PN}_{ij}}} \times 100\% \quad (2)$$

where $\overline{\mathrm{PE}_{ij}}$ denotes the average precipitation of the i station in the j season in a specific ENSO period, and $\overline{\mathrm{PN}_{ij}}$ denotes the average precipitation of the i station in the j season in the normal period.

4. Results

4.1. Distributions of Monthly Precipitation in Different ENSO Years

[16] In order to study how ENSO events influence precipitation, the averages of monthly precipitation in ENSO year (EPW, CPW, and EPC) and a year after the ENSO year were analyzed and compared with the averages of monthly precipitation in and after the normal year. It should be noted that the first month of a year defined in this section was March, as March is the beginning of spring in the year in south China.

[17] The normal year and a year after the normal year, both had two peaks of monthly precipitation (Figure 2). The larger peaks both occurred in June, while the smaller ones happened in August. Figure 2 shows that only one peak of monthly precipitation was identified in the EPW year and a year after EPW, respectively. In the EPW year, the peak happened during June and was 15% less than the normal year case; in the year after EPW, the peak was found in June and was 25% larger than the normal year case. In the CPW year, only one peak (41% larger) was found, and lagged 1 month, happening in July instead of June. Double peaks were detected in a year after CPW, and the larger peak was 25% greater. In the CPW year, however, monthly precipitation from April to June was 51%, 30%, and 43% less than those in the normal year. Double peaks were found in the EPC year and a year after EPC. The main peak in EPC year was 17% less than the normal year case and that in a year after EPC was also only 4% larger. According to the above analysis, the peaks of monthly precipitation after EPW and CPW increased, while EPC had a relatively small impact

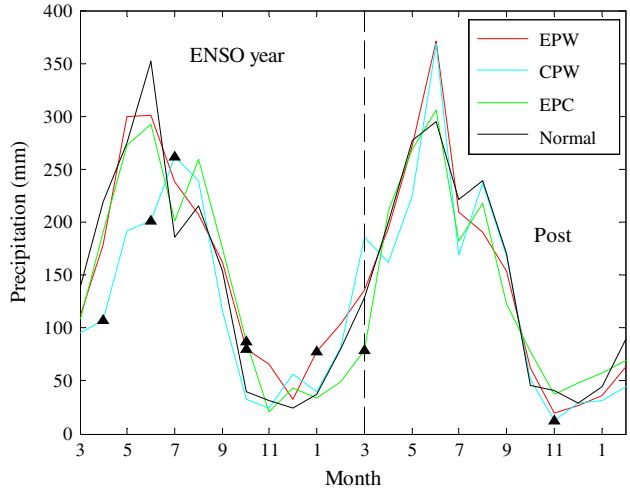

Figure 2. Monthly precipitation in and after ENSO year. The triangle denotes that the distribution of monthly precipitation in that month of that ENSO event is significantly different from the normal condition.

on the peaks of monthly precipitation in a year after EPC. In the EPW, CPW, and EPC years, precipitation in June was less than normal. In the EPW year, however, the precipitation from September to March in the next year was larger than normal. In CPW, precipitation in July and August was larger than normal, while precipitation in most of other months was less than normal. In the EPC year, precipitation in June was less than normal, while precipitation from July to December was larger than normal.

[18] The differences of distributions between the ENSO year and normal year are tested by the Mann–Whitney U test. In EPW year, precipitation in October and January was significantly larger than normal. In CPW year, precipitation in April and June was significantly less than the normal. In EPC year, precipitation in October significantly increased, while that in March significantly decreased.

[19] In this section, it is important to note that the monthly precipitation after ENSO year may also be influenced by the ENSO event in that year. For instance, 1970 is an EPC year, while 1971, a year after 1970, is also an EPC year.

4.2. Anomalies of Seasonal Precipitation

[20] Percentages of seasonal precipitation anomalies were calculated in order to investigate the influences of different ENSO events on seasonal precipitation. In section 4.1, the monthly precipitation in and after different ENSO years are compared with that in and after normal years. However, in this section, the anomalies of seasonal precipitation during different ENSO years and normal years are compared with the climatology, which is denoted by the average of the seasonal precipitation of the considered season during 1956–2005, i.e., the climatology of spring is denoted by the average of the spring precipitation during 1956–2005. Among the total 8 years of EPW events, four of four of them have positive/negative percentages of spring precipitation anomalies, and one of one is larger/lower than 50%/−50% (Figure 3). With respect to CPW case, the percentages were all negative with two of them (40% of the negative percentages) were less than −50%, indicating the comparison with the climatology denoted by the long-term average of spring

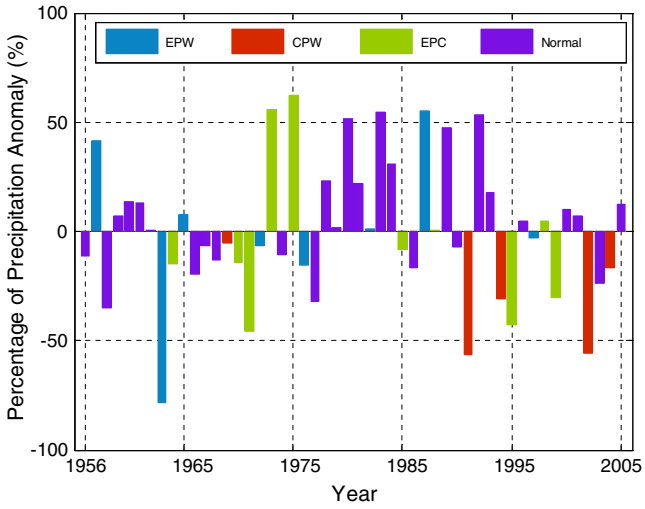

Figure 3. Percentage of precipitation anomalies in spring.

precipitation, CPW triggered less spring precipitation in the East River basin. As for EPC, four of six of the percentages were positive/negative, and two of percentages of negative precipitation anomaly are larger than 50%. The anomalies of normal years are also important and show certain temporal patterns (Figure 3): the period of 1956–1977 is dominated by negative precipitation anomaly; the period of 1978–1995 is dominated by positive precipitation anomaly; and the precipitation anomaly seems to be negative in recent years. Therefore, a rough periodicity is identified.

[21] Figure 4 shows the variations of summer precipitation. It can be seen from Figure 4 that precipitation behaviors are different under the influences of EPW, EPC, and particularly in normal years. When EPW happened, precipitation anomaly was mostly negative, so did the precipitation anomaly in CPW years (Figure 4). In the EPC events, four of the percentages of summer precipitation anomalies were positive, and 6 ones were negative, and in this sense, the precipitation anomaly seemed to be negative in EPC events. Distinctly different temporal properties are evident for summer precipitation during normal years when compared to those for spring precipitation, i.e., the period of 1956–1977 is dominated by positive precipitation anomaly; the period of 1978–1995 is dominated by negative precipitation anomaly; and the precipitation anomaly seems to be mostly positive in recent years. Specifically, in the normal years, the percentages of summer precipitation anomalies of 11 years were positive. Among these years with positive percentages, 2 years (18%) suffered remarkable redundant precipitation, as the percentages of these two years were larger than 50%. On the other hand, 16 of percentages were negative and greater than −50%. Moreover, Figure 4 illustrates that more summer precipitation was found before 1970 and after 1993, while the interval between these periods suffered relatively less summer precipitation. Comparison between Figures 3 and 4 indicated fewer percentages of precipitation anomalies above 50% and no percentage was below 50% in summer.

[22] Percentages of autumn precipitation anomalies are shown in Figure 5. In EPW years, seven of the percentages of autumn precipitation anomalies were positive, and one of them (14%) exceeded 100%. Only one EPW year was found with a negative percentage of autumn precipitation anomalies. Besides, it can be seen from Figure 5 that the percentage of autumn precipitation anomalies seems to be decreasing, which might imply weakening influences of EPW on autumn precipitation. As for CPW, precipitation anomalies are mostly negative, indicating that the CPW events made the autumn precipitation in the East River basin to severely decrease. In EPC years, five of the percentages of autumn precipitation anomalies were positive and three of them (60%) were greater than 50%. While also five of the percentages in EPC years were negative, none of them were less than −50%. In the normal years, however, no distinguishable temporal patterns can be identified (Figure 5). However, negative autumn precipitation anomalies are dominant after 1980s.

[23] As for winter precipitation anomalies (Figure 6), five of the percentages of winter precipitation anomalies in EPW years were positive, and two of them (40%) exceeded 50% (Figure 6). It should be noted that the percentage of winter precipitation anomalies in 1982 almost reached 250%, reflecting abnormal heavy precipitation in winter in that

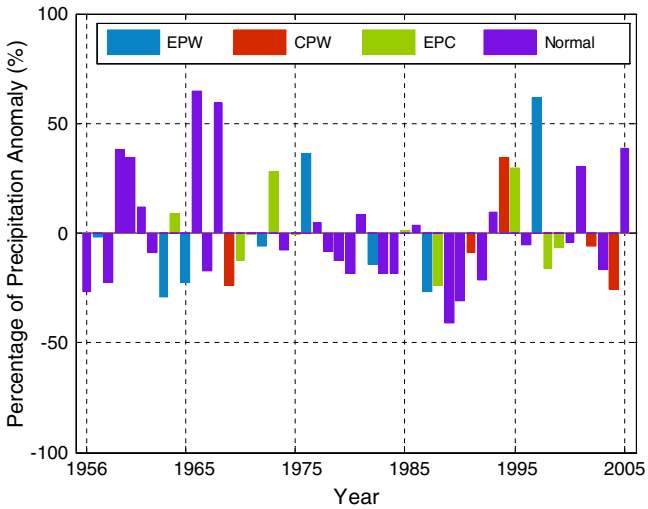

Figure 4. Percentage of precipitation anomalies in summer.

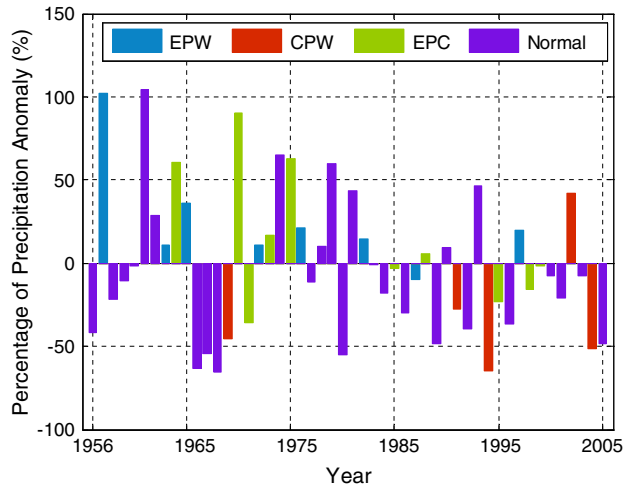

Figure 5. Percentage of precipitation anomalies in autumn.

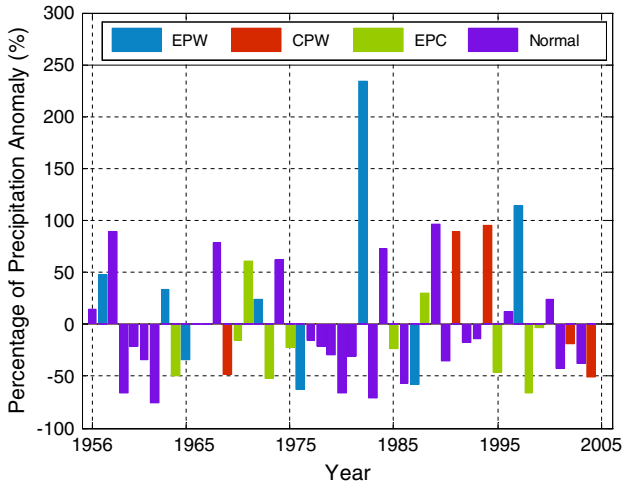

Figure 6. Percentage of precipitation anomalies in winter.

year, which may be the result of an EPW event. On the other hand, three of the percentages in EPW years were negative, and two of them (66%) were below −50%. As for CPW, only two of the percentages were positive, but both of them were greater than 50%. Three of the percentages were negative, and one of them (33%) was less than −50%. Two of the percentages of winter precipitation anomalies in EPC years were positive, and one of them (50%) was larger than 50%. Eight of the percentages in EPC years were negative, while three of them (38%) were less than −50%. In the normal years, 10 years was found with positive percentages, and five of them (50%) had percentages larger than 50%. At the same time, 17 percentages in normal years were negative, and 5 of them (29%) were below −50%.

4.3. Spatial Variations of Seasonal Precipitation in Different ENSO Years

[24] In this section, the precipitation anomaly indices of EPW, CPW, and EPC were interpreted by the inverse distance weighting method. Additionally, the significance of the differences in statistical behavior of precipitation between ENSO years and the normal years was assessed by the Mann–Whitney *U* test. The Mann–Whitney *U* test was applied both to precipitation in stations and the whole region. It should be noted that the precipitation anomaly indices in this section and the percentage of precipitation anomalies in the above section are different. The precipitation anomaly index is the comparison between the precipitation in ENSO years and in normal years, while the percentage of precipitation anomaly is used to compare the precipitation during different ENSO years and normal years with the climatology.

[25] Figure 7 shows the spatial variation of precipitation between EPW and normal years. Negative precipitation anomaly index of EPW in spring was detected in the northern and middle parts of the East River basin, indicating that the spring precipitation in the EPW period was less than in the normal period (Figure 7b). However, the spring precipitation in southwestern parts was larger. In the East River basin, 6 stations had positive precipitation anomaly indices, and 15 ones had negative values, showing that less precipitation in spring was the primary attribute of EPW. Figure 7b shows that the spatial variation of precipitation anomalies in summer was similar to that in spring, besides the region that where it rained less moved southward. Seven stations were detected with positive values, and 14 ones had negative values, indicating that precipitation in summer was also less in EPW. Comparison between Figure 7a and Figure 7b shows that anomalies in summer in the EPC period were smaller those in spring, as the maximum/minimum precipitation anomaly index in spring was 16%/−17%, while the maximum/minimum in summer was only 10%/−11%. In autumn, the variation of precipitation was quite different from that in spring and summer (Figure 7c). Twenty stations were identified with positive precipitation anomalies. Among these 20 stations, 10 stations were detected where the probability distributions in the EPW period differed significantly from those in the normal years. Additionally, the distribution of areal precipitation in the whole East River basin in EPW years was also significantly different from that in the normal years. Thus, more precipitation in autumn in the EPW period was found. The stations with significant difference in the probability distribution of autumn precipitation between EPW and normal periods mainly were located in the middle and northern East River basin. The maximum precipitation anomaly index reached 81%. In winter, it rained more at all 21 stations in EPW years (Figure 7d). When considering annual precipitation, the spatial distribution of precipitation anomaly index was quite similar to that in summer (Figure 7e). Negative values were found at 13 stations located in the northern and middle-eastern parts. The lowest values were found in the middle part. On the other hand, eight positive values of precipitation anomaly index were found in the western and southern parts of the East River basin. Although the number of stations with positive anomalies was less than that with negative anomalies, the largest amplitude of positive precipitation anomaly index was larger than that of negative. Therefore, in the EPW period, it rained less in the middle and northern East River basin, while it rained more in the western and southern East River basin.

[26] Figure 8 shows the spatial variations of precipitation in CPW. As Figure 8a shows, negative precipitation anomaly indices in spring were around the whole East River basin. Seventeen stations were identified having significant differences in the probability distributions of spring precipitation between CPW and normal periods. Moreover, the distribution of areal precipitation in CPW was also different from the normal period. This indicated that CPW made the whole East River basin receive less precipitation in spring. The maximum precipitation anomaly index was −15%, and the minimum reached −54%. In addition, it was found that spring precipitation in middle and southern parts of the East River basin decreased much more severely. Figure 8b illustrates the situations of summer precipitation. Again, less precipitation in CPW was detected in the majority of the East River basin. The number of stations with positive/negative precipitation anomaly index was 4/17. Among the four stations with positive values, one station was identified where the distribution of summer precipitation in CPW altered significantly. On the other hand, much more areas around almost the whole East River basin were detected having negative values. Unlike the spatial distribution of spring precipitation anomaly index, the reduction in summer precipitation was more severe in the middle and northern parts. The East River basin suffered from less

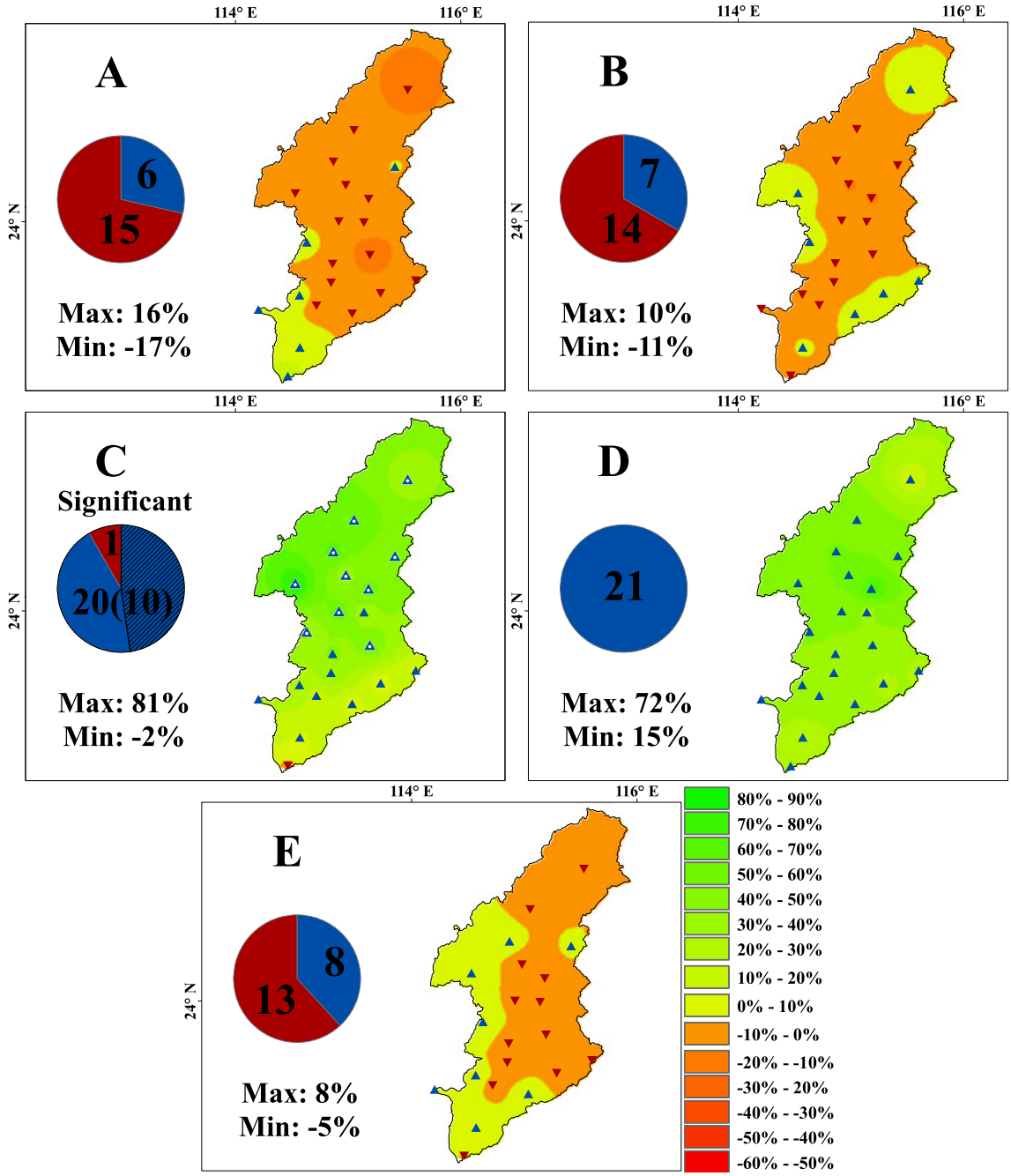

Figure 7. Spatial variations of (a) spring, (b) summer, (c) autumn, (d) winter, and (e) annual precipitation anomaly index of EPW. The green denotes high value, and the red denotes low value. Blue upward triangle denotes station with positive value, and red downward triangle denotes station with negative value. Triangle with white center denotes that the statistical behavior of precipitation of EPW was significantly different from that of normal years. The blue part in the pie bar denotes the number (shown above the pie bar) of stations with positive value, and the red part denotes the number (shown above the pie bar) of stations with negative value. The part with shade denotes the number (inside the bracket) of stations with significant change. The *significant* in Figure 7c denotes that the statistical behavior of areal precipitation of the East River Basin in autumn in EPW was significantly different from that in normal years. The color scale is shown besides Figure 7e.

precipitation in autumn (Figure 8c). The decrease in autumn in the southern East River basin was more serious than in other parts. The minimum value reached −46%, showing the station that had minimum value suffered very severe droughts in CPW. There was an opposite case in winter (Figure 8d). Twenty stations were found with positive precipitation anomaly indices, while only one was with negative value, indicating that there was more precipitation in winter. The largest precipitation anomaly index was 66%. In general, CPW caused less annual precipitation in

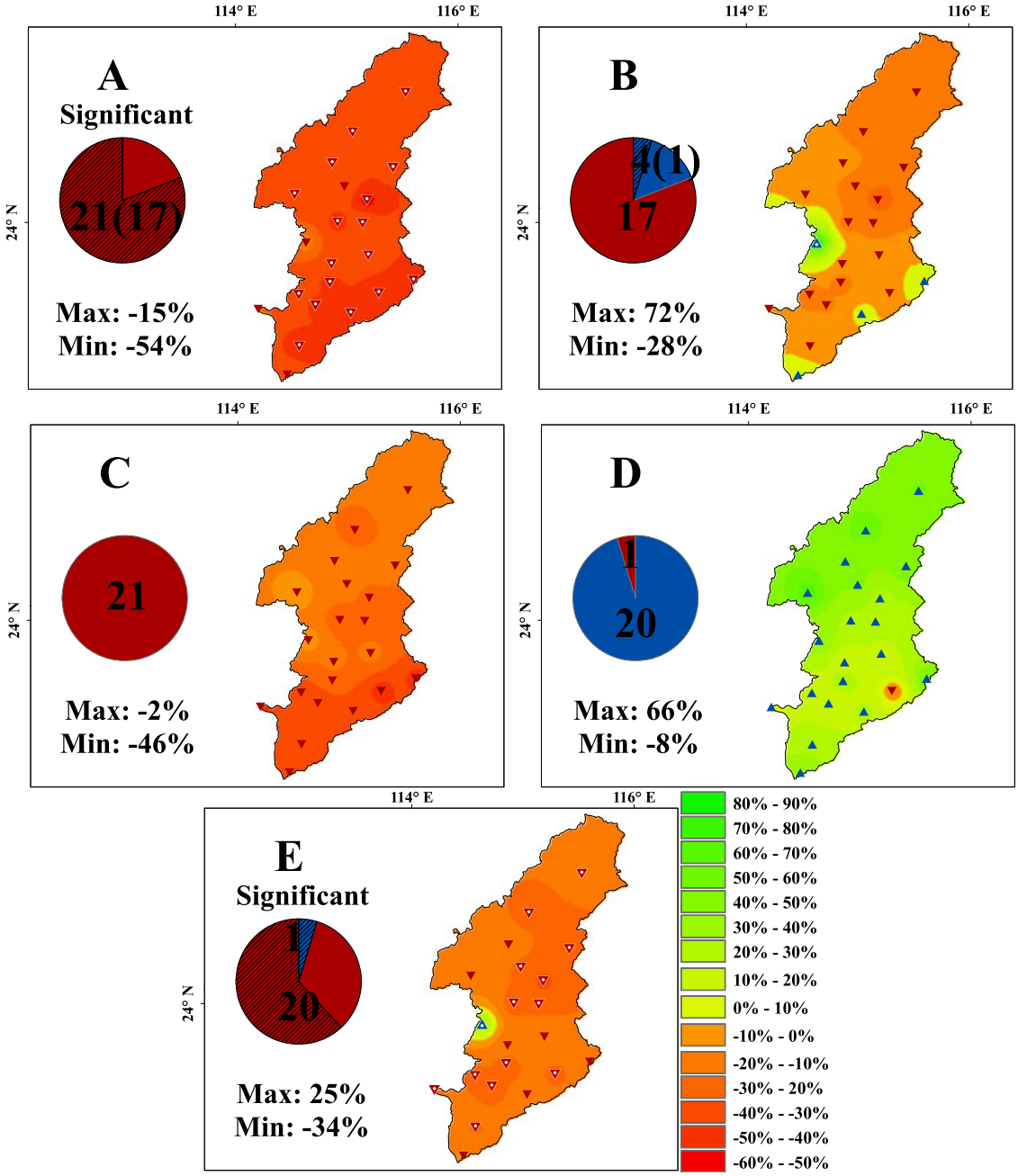

Figure 8. Spatial variations of (a) spring, (b) summer, (c) autumn, (d) winter, and (e) annual precipitation anomaly index of CPW. The instruction is the same as Figure 7.

the whole East River basin, as 20 stations had negative precipitation anomaly index, and 13 of those had significantly different distributions between CPW and normal periods (Figure 8e). In addition, the areal precipitation at the annual scale in CPW also had significantly distinct probability distribution from normal period.

[27] Affected by EPC, there was less spring precipitation in East River basin (Figure 9a). Nineteen stations with negative precipitation anomaly index were found across the whole basin. The minimum value was located in the southern part of the East River basin. In summer, 12 stations had positive precipitation anomaly index, and 9 had negative (Figure 9b). It can be seen that the stations with negative values mainly were in the middle part of the East River basin, while those with positive values were located in the northern and southern parts. The variation of autumn precipitation in EPC was opposite to that in CPW but similar to that in EPW (Figure 9c). More autumn precipitation was found in EPC. Among the 21 stations with positive precipitation anomaly index, three stations had different distributions of precipitation in EPC from normal period. The stations with large precipitation anomaly index were mainly located in the northern East River basin. As for winter, it was the opposite of the autumn case. Less winter precipitation was identified in the EPC years, which was different from the winter case in EPW and CPW (Figure 9d). Like autumn, the stations suffering from most severe precipitation decreases were mainly located in the middle of the

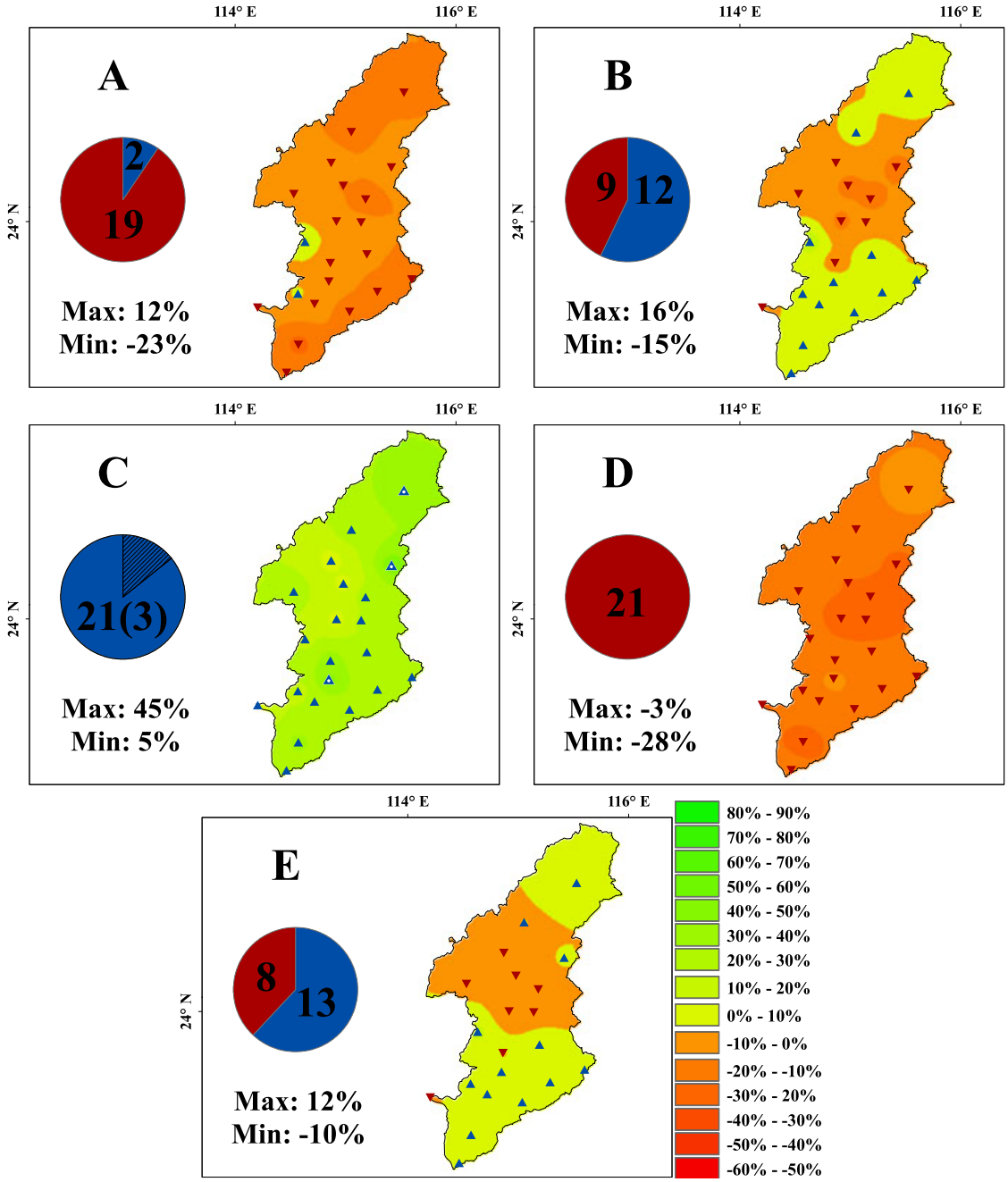

Figure 9. Spatial variations of (a) spring, (b) summer, (c) autumn, (d) winter, and (e) annual precipitation anomaly index of EPC. The instruction is the same as Figure 7.

East River basin. At the annual scale, 13 stations were found with positive precipitation anomaly index, and 8 were found with negative values (Figure 9e). Also similar to the cases in autumn and winter, the area suffering most severe precipitation reduction was located in the middle of the East River basin.

[28] Different places of a relatively small-scale region were under the similar large-scale atmospheric condition with a gradual spatial change, so the spatial difference of precipitation anomalies was also relatively gradual. In addition, due to discrepancy of other factors influencing precipitation, e.g., orography and human influence, the East River basin has obvious spatial patterns of precipitation anomalies.

4.4. Correlation Coefficient Between ENSO Indices and Areal Precipitation

[29] The Pearson correlation coefficient between areal precipitation and ENSO indices, including SSTA of Niño 1 + 2, Niño 3, Niño 4, and Niño 3.4, SOI, and EMI, is illustrated in Figure 10. Here it was investigated as to what the effect of previous ENSO events was following the areal precipitation. Thus, when reading Figure 10, the month of SSTA/SOI/EMI was the month in or before the month of areal precipitation. For example, when referring to the coefficient between areal precipitation in March and SOI in February, areal precipitation in March and SOI in

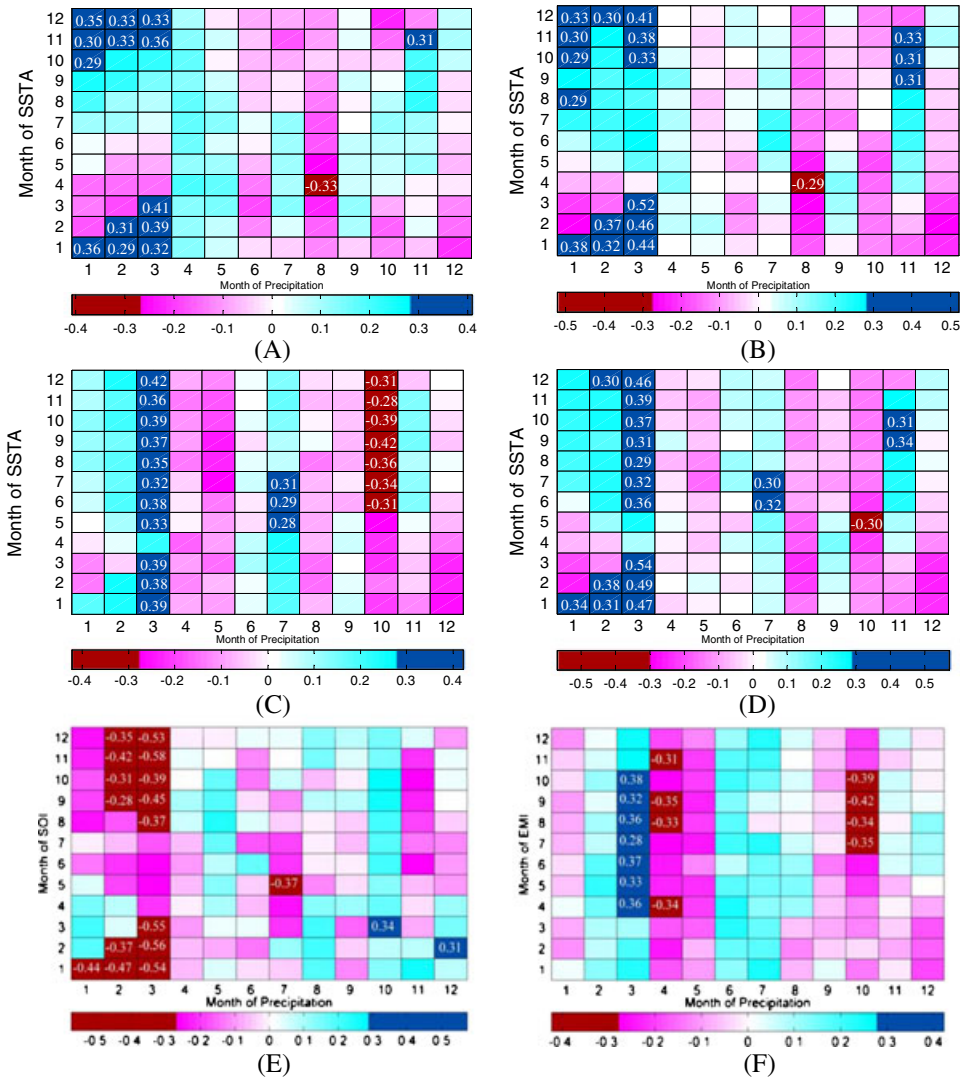

Figure 10. Pearson correlation coefficients between (a) SSTA of Niño 1 + 2 and areal precipitation, (b) SSTA of Niño 3 and areal precipitation, (c) SSTA of Niño 4 and areal precipitation, (d) SSTA of Niño 3.4 and areal precipitation, (e) SOI and areal precipitation, and (f) EMI and areal precipitation. It should be noted that the month of SSTA/SOI/EMI denotes the month that is in or earlier than the month of precipitation. The pink denotes the negative coefficient without significance, and the light blue denotes positive coefficient without significance. The dark red denotes negative coefficient with significance, and the dark blue denotes positive coefficient with significance. The number denotes the specific coefficient with significance.

February in the same year were taken into consideration. When referring to the coefficient between areal precipitation in April and EMI in October, the areal precipitation in April and SOI in October in the previous year were taken into account.

[30] Figure 10a illustrates the Pearson correlation coefficients between SSTA of Niño 1 + 2 and areal precipitation in the East River basin. The areal precipitation in January was significantly and positively influenced by the SSTA of Niño 1 + 2 in January in the same year and in December, November, and October in the previous year. The maximum coefficient was found with SSTA in January, indicating that the precipitation in January in the East River basin was mainly influenced by the SSTA of Niño 1 + 2 in January. As for the areal precipitation in February, it had significant and positive coefficients with SSTA of Niño 1 + 2 in February and January in the same year and in December and November in the previous year. The maximum coefficients were found with SSTA in December and November in the previous year. Precipitation in March was positively impacted by SSTA in March, February, and January in the same year and in December and November in the previous year. SSTA in March had the largest coefficient of 0.41 with precipitation in March. Furthermore, precipitation in August was only influenced negatively by SSTA of Niño 1 + 2 in April in the previous year, and the coefficient was −0.33. The precipitation in November was positively correlated with SSTA in November. For other months, although without significance in some cases, relationships between areal precipitation and SSTA in some months had

some kind of patterns. The areal precipitation in April was always positively influenced by SSTA in all months, and precipitation in August was always affected negatively by SSTA.

[31] Figure 10b shows that the influence of SSTA in Niño 3 on precipitation was similar to that of SSTA in Niño 1 + 2. Precipitation in January was significantly and positively correlated with SSTA in Niño 3 in January in the same year and in December, November, October, and August in the previous year. Precipitation in February was highly and positively correlated with SSTA in February and January in the same year and in December in the previous year. SSTA in Niño 3 in March, February, and January in the same year and December, November, and October in the previous year significantly and positively impacted precipitation in March. Precipitation in March, February, and January had the largest Pearson correlation coefficients with SSTA in March, February, and January, respectively. The coefficient between precipitation and SSTA in March reached 0.52. Precipitation in August only had a significant and negative coefficient with SSTA in Niño 3 in April. Precipitation in November was positively impacted by SSTA in November, October, and September with significance. Furthermore, precipitation in August always had negative relationships with SSTA in Niño 3 in all months.

[32] The correlation between precipitation in the East River basin and SSTA in Niño 4 is shown in Figure 10c. Precipitation in March was positively correlated with SSTA in Niño 4 in all months except April. The Pearson correlation coefficient between precipitation in March and SSTA in Niño 4 in December was the largest. Precipitation in July had a significant and positive correlation with SSTA from May to July. On the other hand, precipitation in October was negatively influenced by SSTA from June to October in the same year and from December and November in the previous year. The minimum coefficient was found between precipitation in October and SSTA in September, indicating higher SSTA in Niño 4 in September and less areal precipitation in the East River basin in October. In addition, precipitation in March was constantly positively affected by SSTA. On the other side, precipitation in May and October was always negatively impacted by SSTA in all months.

[33] The Pearson correlation coefficients between precipitation and SSTA in Niño 3.4 are shown in Figure 10d. Precipitation in January was only positively influenced by SSTA in Niño 3.4 in January with significance. Like Niño 1 + 2 and Niño 3, SSTA in Niño 3.4 in February and January in the same year and in December in the previous year significantly and positively impacted precipitation in February. Precipitation in March was positively influenced with significance by SSTA in Niño 3.4 in all months except April and May. The largest coefficient was between precipitation and SSTA in March. Furthermore, precipitation in July was positively influenced by SSTA in July and June with significance. Precipitation in November was positively affected by SSTA in October and September. Precipitation in October, unlike the relationship with SSTA in Niño 4, was only negatively influenced by SSTA in May with significance. On the other hand, precipitation in March had a positive coefficient with SSTA in Niño 3.4 all the time, while precipitation in August and October was always negatively influenced by SSTA.

[34] Figure 10e depicts the correlations between precipitation and SOI. The coefficient between precipitation and SOI in January was negative and significant. Precipitation in February had significantly negative correlations with SOI in February and January in the same year and in December, November, October, and September in the previous year. The Pearson correlation coefficient between precipitation in February and SOI in January was minimal, with a value of −0.47. Furthermore, SOI in March, February, and January in the same year and in December, November, October, September, and August in the previous year negatively influenced precipitation in March with significance. The Pearson correlation coefficients of SOI from November to March were all below −0.50. The coefficient between precipitation in March and SOI in November in the previous year reached a minimum value of −0.58, meaning higher SOI in November in the previous year and less precipitation in March. The coefficient between precipitation in July and SOI in May was significant and negative. Precipitation in October was positively influenced by SOI in March with significance. Precipitation in November had a significantly positive correlation with SOI in February. As the opposite of the relationship between precipitation and SSTA in Niño 3.4, precipitation in March always had a negative correlation with SOI, and precipitation in October always had a positive correlation with SOI.

[35] Figure 10f shows the correlation between precipitation and EMI. Precipitation in March was positively and significantly influenced by EMI from April to October in the previous year. The largest coefficient was found between precipitation in March and EMI in October in the previous year, indicating higher EMI in October in the previous year and more precipitation in March. Precipitation in April was negatively affected by EMI in April in the same year and in November, September, and August in the previous year. The least coefficient was found between precipitation in March and EMI in September in the previous year. Additionally, precipitation in October was negatively influenced by EMI from July to October. EMI in September had the minimum coefficient with precipitation in October. Moreover, precipitation in March and June was positively influenced by EMI, and precipitation in April, May, and October was always negatively affected by EMI.

5. Discussion

[36] The amount of precipitation over a region is determined to some extent by the available moisture; therefore, transportation of water vapor by the atmospheric circulation plays a vital role in determining rainfall patterns [*Li and Zhou*, 2012]. EPW is defined as an El Niño event excluding the El Niño Modoki in this study. *Chan and Zhou* [2005] indicated that the early summer monsoon rainfall (May–June) tends to be less than normal in the El Niño event over south China. In this paper, the May–June precipitation in EPW was less than normal, which agrees with the results of *Chan and Zhou* [2005] (Figure 2). In the summer of a developing El Niño event, the East Asia Summer Monsoon is weak and below-normal monsoon rainfall is observed in the south China and also the East River basin of this study (Li and Zhou). *Weng et al*. [2008] suggested that southeastern China should be wet in winter during El Niño. It can be seen from Figure 2

that the total precipitation in winter in EPW was above normal. Moreover, according to the percentages of precipitation anomalies (Figure 4), in summer, 75% of the EPW years had negative anomalies, indicating that a reduction in summer precipitation occurred with a high frequency in EPW, which is in agreement with the previous studies [*Chan and Zhou*, 2005; *Zhang et al*., 1999]. On the other hand, it cannot be neglected that EPW may also bring about heavy precipitation in summer, as the anomaly in 1997 exceeds 50%. In winter, EPW brought more precipitation to the East River basin (Figure 6). At the same time, EPW sometimes induced extremely large precipitation anomalies. For example, anomalies in 1982 and 1997 exceeded 200% and 100%, respectively. *Zhang et al*. [1999] concluded that during El Niño, positive precipitation anomalies were identified in southern China in spring, autumn, and winter. In general, the above results support the previous studies. In summer, the reduction in precipitation in EPW was mainly located around the middle part of the East River basin (Figure 7b). The increase in precipitation in autumn and winter was observed over the whole East River basin (Figures 7c and 7d). At the annual scale, the middle and north parts of the East River basin suffered from decreasing precipitation in EPW (Figure 7d).

[37] CPW denotes the El Niño Modoki event. *Weng et al*. [2007] indicated that the East River basin in the southern China did not experience a significant precipitation change in summer during El Niño Modoki. Indeed, the total precipitation in summer in CPW was only −7% less than normal (Figure 2). However, the pattern of summer precipitation in CPW was different from normal. In CPW, it rained significantly less in June, but rained significantly more in July and August. This cannot be identified by only considering the total summer precipitation. *Feng and Li* [2011b] also suggested that south China in spring suffered from a significant reduction in precipitation when El Niño Modoki events happened. Besides, during spring, the subtropical high extends substantially westward during both El Niño and El Niño Modoki years. The high retreats nearly to its climatological location during May and June in El Niño Modoki events. However, the high tends to be sustained until July in El Niño cases. This is in favor of more rainfall in the south China, which is associated with the lower tropospheric western north Pacific anomalous anticyclone [*Feng et al*., 2011a]. According to the percentages of spring precipitation anomalies (Figure 3), the East River basin became drier in CPW, as all percentages of anomalies in CPW were negative. Figure 8a also shows that reduction in spring precipitation was observed across the whole basin. Furthermore, 80% of CPW led to less precipitation in autumn, and induced severe droughts sometimes (Figure 5), and stations detected with decreasing precipitation in autumn were located in the whole basin (Figure 8c). In July and August, the subtropical high associated with western north Pacific anticyclone is intensified with a westward shift. Hence, the southerly wind anomalies on the western side of the anticyclone extend to northern China and bring plentiful moisture to the region from the Huaihe River to the Yellow River, which causes below-normal rainfall in the south China due to the subtropical high [*Feng et al*., 2011a; *Li and Zhou*, 2012]. Usually, CPW is known as an event that decreases precipitation in the southern China in winter [*Weng et al*., 2008]. However, the total precipitation in the East River basin in CPW was slightly larger than normal (Figure 2), and an increase in winter precipitation in CPW was observed around East River basin (Figure 8d). On the other hand, it can be found that CPW also induced heavy precipitation in winter (Figure 6). At the annual scale, CPW made the East River basin drier (Figure 8e).

[38] EPC refers to the La Niña event. *Chan and Zhou* [2005] indicated that the early summer monsoon rainfall (May–June) tended to be larger than normal in La Niña events. The May–June precipitation in the East River basin in EPC, nevertheless, was less than normal, which was in disagreement with Chan and Zhou's study (Figure 2). This difference may be induced by the discrepancy in the study region, as the East River basin is just a part of southern China. According to Figure 9b, many places were detected with more precipitation in summer in EPC. Moreover, EPC brought about more precipitation in autumn (Figures 5 and 9c) and less precipitation in spring and winter (Figures 9a and 9d). In addition, the middle part of the East River basin was the area suffering from the most serious reduction of precipitation in EPC in spring, summer, winter, and the year (Figure 9).

[39] The areal precipitation in the East River basin in February and January had positive correlations with SSTA in Niño 1 + 2, Niño 3, and Niño 3.4 and also had negative correlations with SOI. Areal precipitation in March had positive correlations with SSTA in four regions and EMI and also had negative correlations with SOI. Precipitation in April only had negative correlations with EMI. SSTA in Niño 3 and Niño 3.4 and SOI had significant correlations with precipitation in July. Precipitation in August only had negative relationships with SSTA of Niño 1 + 2 and Niño 3 in April. The areal precipitation in October had negative relationships with SSTA of Niño 3, Niño 3.4, and EMI and positive relationship with SOI in March. Precipitation in November was detected with positive relationships with SSTA of Niño 1 + 2, Niño 3, and Niño 3.4, and precipitation in December only had positive correlation with SOI in February.

6. Conclusions

[40] This paper investigates how different ENSO events influence precipitation in the East River basin from four perspectives: (1) distribution of monthly precipitation, (2) temporal precipitation anomalies in different seasons, (3) spatial variations of seasonal precipitation, and (4) correlation coefficients between areal precipitation and different ENSO indices. The following conclusions are drawn from this paper:

(1) EPW brings more precipitation in autumn and winter for the East River basin but less precipitation in summer. At the same time, EPW may also bring heavy precipitation in summer and extremely heavy precipitation in winter. The whole East River basin becomes wetter in autumn and winter due to EPW. At the annual scale, the middle and north parts of the East River basin experience decreasing precipitation in EPW.
(2) Generally, CPW reduces the precipitation in the whole East River basin in spring, autumn, and the year. Some

heavy precipitation events also happen in winter in CPW. CPW has little impact on the total precipitation in summer, but the pattern of precipitation is altered.

(3) EPC induces more autumn precipitation and less spring and winter precipitation in the East River basin. The middle East River basin gets drier in EPC years.

(4) SSTA of Niño 1 + 2, Niño 3, Niño 4, and Niño 3.4, as well as SOI and EMI are all good indicators of the areal precipitation in the East River basin from January to March. SSTA of Niño 3 and EMI are good indicators of areal precipitation in October. SSTA of Niño 3 and Niño 4 from May to July positively influences precipitation in July. EMI is the only index reflecting precipitation in April.

[41] **Acknowledgments.** This study was supported by the National Natural Science Foundation of China (grant 41071020), Program for New Century Excellent Talents in University (NCET), and the Geographical Modeling and Geocomputation Program under the Focused Investment Scheme (1902042) of The Chinese University of Hong Kong. Our cordial gratitude should be extended to the editor-in-chief, Steve Ghan, and two anonymous reviewers for their pertinent and professional comments which are greatly helpful for further improvement of the quality of this paper.

References

Andrews, E. D., R. C. Antweiler, P. J. Neiman, and F. M. Ralph (2004), Influence of ENSO on flood frequency along the California coast, *J. Climate*, *17*, 337–348.

Ashok, K., S. Behera, A. S. Rao, H. Y. Weng, and T. Yamagata (2007), El Niño Modoki and its possible teleconnection, *J. Geophys. Res.*, *112*, C11007, doi:10.1029/2006JC003798.

Ashok, K., S. Iizuka, S. A. Rao, N. H. Saji, and W. J. Lee (2009), Processes and boreal summer impacts of the 2004 El Niño Modoki: an AGCM study, *Geophys. Res. Lett.*, *36*, L04703, doi:10.1029/2008GL036313.

Chan, J. C. L., and W. Zhou (2005), PDO, ENSO and the early summer monsoon rainfall over south China, *Geophys. Res. Lett.*, *32*, L08810, doi:10.1029/2004GL022015.

Chen, Y. D. (2001), Sustainable development and management of water resources for urban water supply in Hong Kong, *Water Int.*, *26*(1), 119–128.

Chen, Y. D., Q. Zhang, X. Lu, S. R. Zhang, and Z. X. Zhang (2011), Precipitation variability (1956–2002) in the Dongjiang River (Zhujiang River basin, China) and associated large-scale circulation, *Quat. Int.*, *224*(2), 130–137.

Cole, J. E., and E. R. Cook (1998), The changing relationship between ENSO variability and moisture balance in the continental United States, *Geophys. Res. Lett.*, *25*(24), 4529–4532.

Dai, A., and T. M. L. Wigley (2000), Global patterns of ENSO-induced precipitation, *Geophys. Res. Lett.*, *27*(8), 1283–1286.

Eichler, T., and W. Higgins (2006), Climatology and ENSO-related variability of North American extratropical cyclone activity, *J. Climate*, *19*, 2076–2093.

Feng, J., W. Chen, C. Y. Tam, and W. Zhou (2011), Different impacts of El Niño and El Niño Modoki on China rainfall in the decaying phases, *Int. J. Climatol.*, *31*, 2091–2101.

Feng, J., and J. Li (2011), Influence of El Niño Modoki on spring rainfall over south China, *J. Geophys. Res.*, *116*, D13102, doi:10.1029/2010JD015160.

Gelati, E., H. Madsen, and D. Rosbjerg (2011), Stochastic reservoir optimization using El Niño information: case study of Daule Peripa, Ecuador, *Hydrol. Res.*, *42*(5), 413–431.

Kim, H. M., P. J. Webster, and J. A. Curry (2009), Impacts of shifting patterns of Pacific Ocean warming on North Atlantic tropical cyclones, *Science*, *325*, 77–80.

Kumar, K. K., B. Rajagopalan, and M. A. Cane (1999), On the weakening relationship between the Indian monsoon and ENSO, *Science*, *284*, 2156–2159.

Li, X. Z., and W. Zhou (2012), Quasi-4-Yr coupling between El Niño–Southern Oscillation and water vapor transport over East Asia–WNP. *J. Climate*, *25*, 5879–5891.

Mann, H. B., and D. R. Whitney (1947), On a test of whether one of two random variables is stochastically larger than the other, *Ann. Math. Stat.*, *18*(1), 50–60.

Nicholls, N. (1985), Towards the prediction of major Australian droughts, *Aust. Meteorol. Mag.*, *33*, 161–166.

Pardo-Iguzquiza, E. (1998), Comparison of geostatistical methods for estimating the areal average climatological rainfall mean using data on precipitation and topography, *Int. J. Climatol.*, *18*, 1031–1047.

Parry, S., J. Hannaford, B. Lloyd-Hughes, and C. Prudhomme (2012), Multi-year droughts in Europe: analysis of development and causes, *Hydrol. Res.*, *43*(5), 689–706.

Pielke, Jr. R. A., and C. N. Landsea (1999), La Niña, El Niño, and Atlantic hurricane damages in the United States, *Bull. Am. Meteorol. Soc.*, *80*(10), 2027–2033.

Power, S., T. Casey, C. Folland, A. Colman, and V. Mehta (1999), Inter-decadal modulation of the impact of ENSO on Australia, *Clim. Dyn.*, *15*, 319–324.

Ratnam, J. V., S. K. Behera, Y. Masumoto, K. Takahashi, and T. Ymagata (2012), Anomalous climatic conditions associated with the El Niño Modoki during boreal winter of 2009, *Clim. Dyn.*, *39*(1–2), 227–238.

Skaugen, T., H. B. Stranden, and T. Saloranta (2012), Trends in snow water equivalent in Norway (1931–2009), *Hydrol. Res. 43*(4), 489–499.

Smith, T. M., and R. W. Reynolds (2004), Improved extended reconstruction of SST (1854–1997), *J. Climate*, *17*, 2466–2476.

Smith, T. M., R. W. Reynolds, T. C. Peterson, and J. Lawrimore (2008), Improvements to NOAA's historical merged land-ocean surface temperature analysis (1880–2006), *J. Climate*, *21*, 2283–2296.

Taschetto, A. S., and M. H. England (2008), El Niño Modoki impacts on Australian rainfall, *J. Climate*, *22*, 3167–3174.

Wang, B., R. Wu, and X. Fu (2000), Pacific-East Asian teleconnection: how does ENSO affect East Asian climate? *J. Climate*, *13*, 1517–1536.

Weng, H., K. Ashok, S. K. Behera, S. A. Rao, and T. Yamagata (2007), Impacts of recent El Niño Modoki on dry/wet conditions in the Pacific rim during boreal summer, *Clim. Dyn.*, *29*(2-3), 113–129.

Weng, H., S. K. Behera, and T. Yamagata (2008), Anomalous winter climate conditions in the Pacific rim during recent El Niño Modoki and El Niño events, *Clim. Dyn.*, *32*(5), 663–674.

Wrzesi ski, D., and R. Paluszkiewicz (2011), Spatial differences in the impact of the North Atlantic Oscillation on the flow of rivers in Europe, *Hydrol. Res.*, *42*(1), 30–39.

Zhang, R., S. Akimasa, and K. Masahide (1999), A diagnostic study of the impact of El Nino on the precipitation in China, *Adv. Atmos. Sci.*, *16*(2), 229–241.

Zhang, Q., V. P. Singh, and J. Li (2012a), Eco-hydrological requirements in arid and semi-arid regions: the Yellow River in China as a case study, *J. Hydrol. Eng.*, doi:10.1061/(ASCE)HE.1943-5584.0000653.

Zhang, Q., V. P. Singh, J. Li, F. Jiang, and Y. Bai (2012b), Spatio-temporal variations of precipitation extremes in Xinjiang, China, *J. Hydrol.*, *434–435*, 7–18.

Zhang, Q., C. Y. Xu, T. Jiang, Y. Wu (2007), Possible influence of ENSO on annual maximum streamflow of the Yangtze River, China, *J. Hydrol.*, *333*, 265–274.

Zou, K. H., K. Tuncali, and S. G. Silverman (2003), Correlation and simple linear regression, *Radiology*, *227*, 617–628.